21st Australasian Fluid Mechanics Conference
Adelaide, Australia
10-13 December 2018

Empirical scaling analysis of jet control using unsteady minijet

Perumal. A. K[1,3] and Zhou. Y[1,2]
[1]Institute for Turbulence-Noise-Vibration Interactions and Control,
Harbin Institute of Technology, (Shenzhen), China
[2]Digital Engineering Laboratory of Offshore Equipment, Shenzhen, China
[3]Indian Institute of Technology Jammu, Jammu, India.

Abstract

This work presents the active control of a turbulent axisymmetric jet using single unsteady minijet. The forcing parameters include the ratio f_e/f_0 of the minijet excitation frequency f_e to the main jet preferred-mode frequency f_0, duty cycle (α) the fraction of time the minijet is "on" during each pulsation cycle, the mass flow rate ratio C_m of the minijet to the main jet, and the exit diameter ratio d/D of the minijet to main jet. The jet centerline velocity decay rate K is used to evaluate jet entrainment rate, given by an equation of $K = (\overline{U}_e - \overline{U}_{5D})/\overline{U}_e$, where U_e and U_{5D} denote the jet centerline mean velocities at $x^* = x/D = 0$ and 5, respectively. Extensive hot-wire measurements were performed in the injection, orthogonal non-injection planes of the perturbed jets.

Introduction

Jet mixing manipulation is of great importance in combustion, heat transfer and noise reduction, and thus has extensive practical applications in industries, including heating or combustion chambers, ejectors, spraying, aircraft engine, metal deposition, electronic equipment cooling and drying. Over the past few decades, many techniques have been proposed to improve the jet effectiveness either passively or actively. Passive techniques such as tabs (e.g. Bradbury & Khadem [2]), non-circular nozzles (e.g. Husain & Hussain [7]) and chevron nozzles (e.g. Zaman *et al.* [12]) are highly effective, though carrying with them certain penalties, for example, thrust loss, drag, practical constraints (e.g. Gutmark & Grinstein [6]). On the other hand, active methods require the input of external power, e.g. acoustic excitation (e.g. Zaman & Hussain [13]), piezo-electric actuators (e.g. Wiltse & Glezer [8]) and plasma actuators (e.g. Samimy *et al.* [9]).

Recently, one active technique has attracted considerable attention in the literature, which uses minijet, also referred to as the secondary jet, fluidic means or air-tab, as the actuator. This technique can be easily adapted to the flow conditions and will not cause thrust loss. In fact, the minjet can be turned on and off depending on practical needs and this has encouraged many researchers to explore this option for jet mixing and noise control. The concept to use fluidic injection for enhancing jet mixing was first proposed by Davis [3] on a Mach 0.8 jet. This technique may reproduce the same benefits of the solid tabs (e.g. Behrouzi *et al.* [1]).

The minijet injection can be significantly more efficient if made pulsed (e.g. Freund & Moin [4]). Previous investigations on jet control using unsteady fluidic means are mostly focused on the mass flow rate and frequency ratios, i.e. C_m and f_e/f_0, of the minijet to main jet (e.g. Behrouzi *et al.* [1] and Yang *et al.* [11]), where f_e and f_0 are the excitation frequency of the unsteady minijet and the preferred mode frequency of the main jet, respectively. Yang & Zhou [10] and Yang *et al.* [11] conducted detailed investigations on the effect of C_m and f_e/f_0 on a turbulent round jet (Re = 8000) manipulated by two symmetrically or asymmetrically arranged unsteady minijets, respectively.

Previous studies have improved tremendously our understanding of jet control based on unsteady minijets. Nevertheless, a systematic parametric study in this area is missing in the literature. For instance, there is another parameter, namely the duty cycle α, associated with unsteady minijets, that is available for optimizing the control performance (e.g. Johari *et al.* [5]). There has been so far no study on its influence on the jet control performance. Furthermore, the effect of the diameter ratio d/D, where d is the minijet exit diameter, has not been thoroughly understood either although Davis [3] pointed out a decrease in d/D may improve the control efficiency. Realizing jet entrainment or mixing may depend on C_m, f_e/f_0, α and d/D, viz. the decay rate of the jet centerline mean velocity $K = g\ (C_m, f_e/f_0, \alpha, d/D)$, we are faced an important issue, that is, could we obtain from C_m, f_e/f_0, α and d/D the similarity variables that reflect the physical essence of the jet control and can be used to design minijet in full-scale practical applications? Could we find a scaling factor ξ so that $K = g_1\ (C_m, f_e/f_0, \alpha, d/D)$ may be reduced to $K = g_2\ (\xi)$, where g_1 *and* g_2 are different functions? This may have a profound impact upon possible practical applications since the flow structure and the similarity parameters obtained from a laboratory-scaled model are the same as those of a full-scaled model.

This study sets out to address the above issue raised. A turbulent axisymmetric jet is experimentally manipulated using a single unsteady minijet. Extensive measurements are conducted using hot-wire in the three orthogonal planes of the manipulated jet.

Experimental Details

Experimental rig is deployed in a spacious air-conditioned laboratory whose room temperature is maintained to be constant with a maximum variation of ±0.5°C. The rig is centrally placed in an area of around 4.5 m in width and 4.0 m in height. Careful measures are taken to ensure no external disturbance to the flow by any means during experiments since the jet is highly sensitive to the background noise.

The rig consists of a main jet and a minijet assembly (Figure 1). The compressed air for the main or primary jet and minijet comes from three air tanks connected in series, with a total storage capacity of 8m^3 and a pressure of 12 MPa, which is sufficient for 3 hours in running time. The air supply to the main jet and the minijet is controlled by separate valves. The compressed air is mixed with seeding particles in the pre-mixing and mixing chamber in the case of PIV or flow visualization measurements and then enters a plenum chamber, consisting of a 300-mm-long diffuser of 15 degrees in half angle and a 400 mm-long cylindrical settling chamber with an inner diameter of 114 mm. The flow goes through two wire-mesh screens before entering into the smooth contraction nozzle. The profile of the nozzle contraction is identical to that used in Yang & Zhou [10]. The contraction is extended with a 47-mm-long smooth tube, whose inner diameter is the same as the nozzle exit diameter D (= 20 mm).

The main jet nozzle is drilled with six holes of diameter d, separated azimuthally by 60 degrees and located 17 mm upstream of the main jet exit. Three nozzles, d = 0.5, 0.8 and 1.0 mm, respectively, are made and exchangeable. Each hole is connected via a short plastic hose to an electromagnetic valve

(Koganei K2-100SF-09-LL) with its maximum frequency of 1 kHz, which is used to generate unsteady minijet. The 6 electromagnetic valves are controlled independently. In this study, only one single minijet is used, which is shaded in Figure 1. The valve is driven by a square-wave voltage signal of 0 - 5V from the output board of a NI system and its α may vary from 0.1 to 1.0. The f_e and α of the minijet can be adjusted by changing the frequency and duty cycle of the square wave signal. The frequency range that can be achieved is 0 – 1 kHz. Mass flow rates of both main jet and minijet are adjustable independently via two separate mass flow meters, whose measurement uncertainty is no more than ±1%.

The coordinate system (x, y, z) and its origin O are defined in Figure 1. Measurements were conducted in the minijet injection (x-z) plane, the orthogonal or non-injection (x-y) plane, and at a number of cross-sectional planes (y-z) of the main jet. The instantaneous velocities are denoted by U, V and W along x, y and z, respectively, and their fluctuating components are given by u, v, and w, respectively.

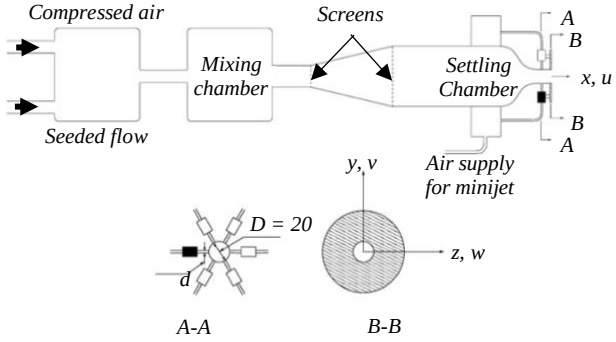

Figure 1. Schematic of experimental rig, minijet assembly and the definition of the coordinate system.

Flow Measurements and Data Processing

The U is measured using a single tungsten wire of 5μm in diameter, operated on a constant temperature circuit (Dantec Streamline) at an over-heat ratio of 1.8. The signal from the wire is offset, filtered at a cut-off frequency of 3kHz, amplified and then digitized using a 12-bit A/D board at a sampling frequency of 6kHz. The record duration is 80s, which ensures that u_{rms} is converged to within 1% uncertainty, where subscript rms denotes the root mean square value. The hotwire probe is mounted on a computer-controlled three-dimensional traversing mechanism, whose streamwise and transverse resolutions are 0.01mm. The hotwire signal is calibrated based on the streamwise mean velocity measured using a standard Pitot static tube with an outer diameter 2.2 mm, connected to an electronic micro manometer (Furness FCO510) and placed, side by side with the hotwire, parallel to the flow near the center of the nozzle exit.

Experimental rig is deployed in a spacious air-conditioned laboratory whose room temperature is maintained to be constant with a maximum variation of ±0.5°C. Experiments were conducted for a jet Reynolds number $\mathrm{Re} \equiv \bar{U}_j D/\nu$ of 8000, where ν is the kinematic viscosity of air. The dynamics viscosity was calculated using Sutherland formula. The power spectral density functions E_u of u measured on the centreline over x^* = 2-6 exhibit a pronounced peak at f_0 = 135 *Hz*, suggesting the occurrence of preferred-mode structures. In this paper, asterisk denotes normalization by the nozzle exit diameter D and/or time-averaged exit velocity $\bar{U}_j$ of the main jet.

Following Zhou *et al.* [14] and Yang & Zhou [10], $K = (\bar{U}_j - \bar{U}_{5D})/\bar{U}_j$ is used to evaluate the jet entrainment rate, where $\bar{U}_{5D}$ denotes the jet centreline mean velocity at $x^* = 5$. Zhou *et al.* [14] defined K is correlated approximately linearly with an equivalent jet half width $R_{eq} = [R_H R_V]^{1/2}$, where R_H and R_V are the jet half-widths in two orthogonal planes, that is, K is directly connected to the entrainment rate of the manipulated jet.

Results and discussion

In general, the decay rate of the jet depends on C_m, f_e/f_0, α and d/D, viz. $K = g\,(C_m, f_e/f_0, \alpha, d/D)$. Could we find a scaling factor ξ so that $K = g_1\,(C_m, f_e/f_0, \alpha, d/D)$ may be reduced to $K = g_2\,(\xi)$, where g_1 *and* g_2 are different functions?

Empirical Scaling of Jet Decay Rate

In this section, an empirical scaling analysis is performed for the jet decay rate in order to find a scaling factor ξ so that $K = g_1\,(C_m, f_e/f_0, \alpha, d/D)$ may be reduced to $K = g_2\,(\xi)$. Valuable insight into the flow control physics behind the influence of the minijet parameters on the flow development may be gained out of this analysis

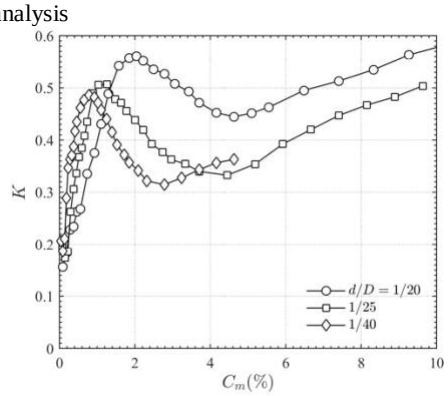

Figure 2: Dependence on d/D on the jet centreline mean velocity decay rate K ($f_e/f_0 = 0.5$, $\alpha = 0.1$

As it is clear in Figure 2, the dependence of K on C_m ($f_e/f_0 = 0.5$ and $\alpha = 0.1$) remains unchanged qualitatively as d/D varies and may be divided into two regimes, i.e., a rapid rise to a local maximum K followed by a drop (Regime I) and then a monotonic growth with increasing C_m (Regime II).Given the same C_m, the minijet velocity increases as d/D is reduced. Physically, the penetration depth of the minjet is determined by the combined effect of the minijet mass flow rate and the minijet exit velocity, that is, the momentum of the minijet plays an important role in determining the overall effectiveness in jet manipulation. After careful physical analysis of the experimental data in Figure 2 along with many trial-and-error attempts, it has been found that the re-scaled K or $K(D/d)^{0.25}$ collapses reasonably well in Regime I for various d/D (Figure 3a) provided that the abscissa is given in terms of the momentum ratio $MR = \frac{\dot{m}_m \bar{U}_m}{\dot{m}_j \bar{U}_j}$ of the minijet to main jet, where $\dot{m}$ and $\bar{U}$ represent the jet mass flow rate and exit velocity, respectively, and subscripts m and j denote minijet and main jet, respectively. MR can be further written as $= \left(\frac{\dot{m}_m}{\dot{m}_j}\right)^2 \frac{\rho_j}{\rho_m}\frac{A_j}{A_m}$, where ρ and A are the density of fluid (air) and the exit area of the minijet or nozzle exit, respectively. For incompressible flow, $MR = \left(\frac{\dot{m}_m}{\dot{m}_j}\right)^2 \left(\frac{D}{d}\right)^2 = C_{\dot{m}}^2 \left(\frac{D}{d}\right)^2$. The result indicates that $\sqrt{MR}$ is the controlling scaling factor. The dependence of $K(D/d)^{0.25}$ on $\sqrt{MR}$ for d/D = 1/20 does not collapse for $\sqrt{MR} > 1.0$ with those for d/D = 1/25 and 1/40. This is because the injected flow through the minijet nozzle of very small diameter ($d/D \le 1/25$) may have been partially choked at

a large C_m, thus resulting in a K value smaller than that expected.

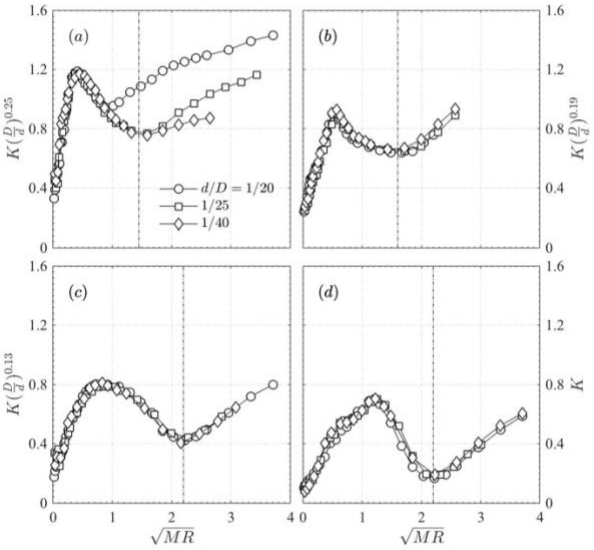

Figure 3: Dependence of the re-scaled centreline mean velocity jet decay rate on $\sqrt{MR}$ (f_e/f_0 = 0.5, α = 0.1); (a) α = 0.1, (b) 0.3, (c) 0.5, (d) 0.9.

A similar collapse is obtained for α = 0.3, 0.5 and 0.9 (Figure 3*b-d*), though the measured K is now re-scaled to $K(D/d)^{0.19}$, $K(D/d)^{0.13}$ and $K(D/d)^{0.00}$, respectively. As a matter of fact, this collapse is well observed for Regime II as well as Regime I since the choking phenomenon may not occur for α ≥ 0.3 in the present experimental conditions. Apparently, the power index n depends on α, which are interestingly linearly correlated by $n = C\alpha + 0.28$ for α = 0.1 - 0.9, where C is -0.31 (Figure not shown). As such, we may write $K\left(\frac{D}{d}\right)^n = g_3\left(\sqrt{MR}\right)$, where n = - 0.31α + 0.28. Note that $n <$ 0.06 for α > 0.7, that is, n is approximately zero, as shown in Figure 4, and the corresponding minijet injection may be referred to as the quasi-steady injection.

A careful analysis along with numerous trial-and-error attempts at least-squares-fitting the data in Regime I indicates that the relationship between $K\left(\frac{D}{d}\right)^n$, $\sqrt{MR}$ and α may be written as

$$K\left(\frac{D}{d}\right)^n = g_4\left(\frac{\sqrt{MR}}{\alpha}\right) \qquad (1)$$

where $\frac{\sqrt{MR}}{\alpha} = \frac{C_m}{\alpha}\frac{D}{d}$ is physically the momentum per pulse of injection. Apparently, for a given minijet diameter and C_m, an increase in α results in a reduced momentum per pulse of injection and subsequently a reduced penetration depth into the main jet, and hence K decreases. On the other hand, for given C_m and α, a decrease in the minijet diameter results in increased $\frac{\sqrt{MR}}{\alpha}$ or penetration depth and hence a higher K provided that the choking phenomenon is absent.

In order to determine g_4, we plot $K\left(\frac{D}{d}\right)^n$ against $\frac{\sqrt{MR}}{\alpha}$ (not shown), which displays a collapse of the data and is approximately piecewise linear, albeit branched. Therefore, the data are replotted in Figure 4 showing the dependence of K on $\frac{\sqrt{MR}}{\alpha}\left(\frac{d}{D}\right)^n$. All the data are from Regime I or the left-hand side of the vertical broken line in Figure 3, with the additional data of α = 0.7. The data of K display a quite good collapse up to $\xi \equiv \frac{\sqrt{MR}}{\alpha}\left(\frac{d}{D}\right)^n \approx 1.0$ but branch into four, i.e. B_1, B_2, B_3 and B_{12} for $\xi > 1.0$. The data are piecewise least-squares-fitted to linear curves, viz.

$K = 0.42\xi + 0.1$ for $0 \le \xi \le$ 1.0-1.5 (depending on α and d/D) (2-1)

B_1: $K = -0.45\xi + 1.37$ for $\xi > 1.5$ (2)

B_2: $K = -0.12\xi + 0.65$ for $\xi > 1.0$ (3)

B_3: $K = -0.07\xi + 0.62$ for $\xi > 1.0$ (4)

B_{12}: $K = -0.36\xi + 1.05$ for $\xi > 1.0$ (5)

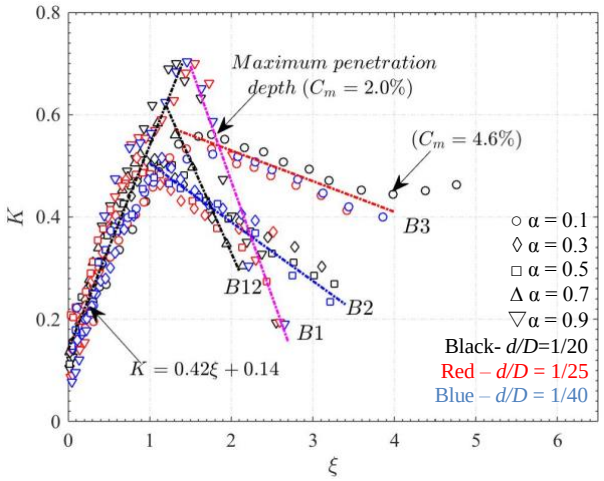

Figure 4 Dependence of the centreline mean velocity jet decay rate K on $\xi = \frac{\sqrt{MR}}{\alpha}\left(\frac{d}{D}\right)^n$ where n = 0.25 - 0. All the data are from the left-hand side of the local peak line in Figure 3.

The measured K may deviate from the calculation from Eq. (2) by no more than 10%, with a 95% confidence; the only exception is $\xi < 0.2$ where the deviation may go up to ±15%.

Before discussing the results in Figure 4, we need to understand physically $\left(\frac{d}{D}\right)^n$. Take the case of d/D = 1/20 and 1/40 for example. As d/D is reduced from 1/20 to 1/40, C_m required to achieve a predefined K, say 0.3, should be less based on Figure 4. We define a percentage reduction by

$$\Delta C_{m\,d/D} = 1 - \frac{[C_m]_{1/40}}{[C_m]_{1/20}}, \qquad (6)$$

where subscripts 1/40 and 1/20 denote diameter ratios (d/D). The required C_m for given K, α and d/D can be calculated from equation (2-1):

$$K \approx \frac{\sqrt{MR}}{\alpha}\left(\frac{d}{D}\right)^n \approx \frac{C_m}{\alpha}\left(\frac{D}{d}\right)^{1-n}, \qquad (7)$$

or

$$C_m \approx K\alpha\left(\frac{d}{D}\right)^{1-n}. \qquad (8)$$

Then $\Delta C_{m\,d/D}$ can be obtained by substituting Eq (8) into (6) for the corresponding d/D. A decrease in d/D by half results in a drop in the required C_m by about half ($\Delta C_{m\,d/D} \approx$ 50%) for α ≥ 0.7. $\Delta C_{m\,d/D}$ contracts to 0.4 or 40% for α = 0.1. The fact that additional C_m, proportional to $(d/D)^{-n}$ (Eq 8), is required to achieve a given K due to a reduced d/D is physically due to the increased retardation effect of the minijet nozzle. A reduction in α further amplifies this retardation effect. That is, $\left(\frac{d}{D}\right)^{-n}$ reflects physically the retardation effect in case of small d/D or α.

Some interesting inferences can be made from Eqs. (2-5). Firstly, given C_m, f_e/f_0, d/D and α (thus n), ξ may be calculated and hence K can be predicted from the equations. This may have important applications in engineering. Secondly, the required C_m to achieve a pre-specified K can be estimated from the equation 2. C_m is a practically important parameter. Following Eq (6), we may define a percentage reduction as α reduces, viz.

$$\Delta C_{m\,\alpha} = 1 - \frac{[C_m]_{0.1-0.8}}{[C_m]_{0.9}}, \qquad (9)$$

where subscripts 0.1-0.8 and 0.9 denote α. A large ΔC_{m_α} means a higher control efficiency. For example, to achieve a pre-determined K = 0.3 for d/D= 1/40, C_m required may be calculated from Eq. (2), which is 0.25% at α = 0.1, 68% lower than that (C_m = 0.80%) at α = 0.9 calculated from Eq. (9). The result highlights the highly effective entrainment under the unsteady minijet excitation of small α. Lastly, as noted earlier, the required C_m drops as d/D is reduced, also implying an improved control efficiency.

Conclusions

Experimental study has been carried out to study the manipulation of a turbulent round jet with a single unsteady minijet. Four control parameters, i.e. C_m, f_e/f_0, α and d/D, are examined to understand their influence on the main jet. Extensive measurements are performed in three orthogonal planes of the main jet. The scaling analysis of the jet control is also performed empirically. Following conclusions are drawn from the investigation:

Empirical scaling analysis has demonstrated that, given a large α say 0.9, the main jet behaves as quasi-steady blowing and the dependence of the measured K on the momentum ratio $\sqrt{MR} = C_m \frac{D}{d}$ of the minijet to main jet collapses for various d/D, that is, $\sqrt{MR}$ is the controlling scaling factor. Once α is reduced to below 0.9, K varies with d/D, but the dependence on $\sqrt{MR}$ of the re-scaled K, i.e., $K(D/d)^n$, again collapses for various d/D; so does the dependence on f_e/f_0 of $K(D/d)^n$. The power index n is dependent only on α and may be given by n = - 0.31α + 0.28 for the present flow and control conditions. Thus, $K = g_1$ (C_m, f_e/f_0, α, d/D) is reduced to one similarity parameter, $\xi = \frac{\sqrt{MR}}{\propto}\left(\frac{d}{D}\right)^n$, where dimensionless parameters $\frac{\sqrt{MR}}{\propto}$ and $(D/d)^n$ are physically the momentum per pulse of the minijet and the resistance/retardation to fluid flowing though the minijet nozzle, respectively. For α ≥ 0.7, $n \approx 0$, that is, the retardation effect is negligibly small. For unsteady injection, this retardation increases with a decrease in d/D as the C_m required to achieve a pre-determined K is simply governed by $\sqrt{MR}$ or (D/d) for α ≥ 0.7 but $\sqrt{MR}\ (d/D)^n$ for α < 0.7. For example, a decrease in d/D by half results in a decrease in the required C_m by 50% for α ≥ 0.7 but a decrease in C_m by 40%, rather than 50%, for α = 0.1. The fact that some additional C_m, proportional to $(d/D)^{-n}$, is required to achieve a pre-defined ξ is physically due to the retardation effect.

Given ξ or K, the required C_m drops as the duty cycle or the minijet injection diameter is reduced, that is, the control efficiency is improved. For example, a 68% reduction in required C_m is achieved at α = 0.1 compared to that at α = 0.9, which highlights the highly effective entrainment under the unsteady minijet excitation of small α; a decrease in d/D by half results in a decrease in the required C_m by 40% (α = 0.1), that is, the choice of d/D may have an important impact upon jet mixing. The penetration depth, flow structure and its downstream development are found to be the same, irrespective of different C_m and d/D, as long as ξ is unchanged. The required momentum ratio or C_m at given d/D and α to achieve a pre-determined ξ or K can be calculated from the scaling relation (Figure 4).

Acknowledgements

YZ wishes to acknowledge support given to him from NSFC through grants 11632006 and U1613226 and AKP acknowledges the support from Research Grants Council of Shenzhen Government through grant JCYJ20160531193220561.

References

[1] Behrouzi, P., Feng, T., & McGuirk, J. J. 2008. Active flow control of jet mixing using steady and pulsed fluid tabs. *Proceedings of the Institution of Mechanical Engineers, Part I: Journal of Systems and Control Engineering*, **222**, 381-392.

[2] Bradbury, L. J. S., & Khadem, A. H., 1975. The Distortion of a Jet by Tabs. *J. Fluid Mech*, **70**, 801–813.

[3] Davis, M. 1982 Variable control of jet decay. *AIAA J.* **20**, 606-609.

[4] Freund, J. B., & Moin, P. 2000. Jet mixing enhancement by high-amplitude fluidic actuation. *AIAA journal*, **38**, 1863-1870.

[5] Johari, H., Pacheco-Tougas, M., & Hermanson, J. 1999. Penetration and mixing of fully modulated turbulent jets in crossflow. *AIAA Journal*, **37.** 842-850.

[6] Gutmark, E. & Grinstein F. 1999 Flow control with noncircular jets. *Annu. Rev. Fluid Mech*. **31**, 239-272.

[7] Husain, H. S & Hussain, A. K. M. F. 1983 Controlled excitation of elliptic jets. *Phys. Fluids*, **26**, 2763-2766

[8] Wiltse, J. M. & Glezer, A. 1993 Manipulation of free shear flows using piezoelectric actuators. *J. Fluid Mech.* **249**, 261-285.

[9] Samimy, M., Kim, J-H., Kastner, J., Adamocich I. & Utkin, Y. 2007 Active control of high-speed and high-Reynolds-number jets using plasma actuators. *J. Fluid Mech*. **578**, 305-330.

[10] Yang, H., & Zhou, Y. 2016. Axisymmetric jet manipulated using two unsteady minijets. *Journal of Fluid Mechanics*, **808**, 362-396.

[11] Yang, H., Zhou, Y., So, R. M. C. & Liu, Y. 2016 Turbulent jet manipulation using two unsteady azimuthally separated radial minijets. *Proc. R. Soc. A* **472**, 20160417.

[12] Zaman, K. B. M. Q., Bridges, J. E., & Huff, D. L. 2011. Evolution from 'tabs' to 'chevron technology'-a review. *International Journal of Aeroacoustics*, **10.** 685-709.

[13] Zaman K. B. M. Q. & Hussain A. K. M. F, 1981 Turbulence suppression in free shear flows by controlled excitation. *J. Fluid Mech*., **103**, 133-159

[14] Zhou, Y., Du, C., Mi, J. & Wang, X. 2012 Turbulent round jet control using two steady minijets. *AIAA J*. **50**, 736-740.